Neurobiology of Stress 30 (2024) 100628

Contents lists available at ScienceDirect

Neurobiology of Stress

journal homepage: www.elsevier.com/locate/ynstr

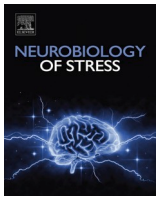

β1-adrenoceptor expression on GABAergic interneurons in primate dorsolateral prefrontal cortex: potential role in stress-induced cognitive dysfunction

M.K.P. Joyce, S. Yang, K. Morin, A. Duque, J. Arellano, D. Datta, M. Wang, A.F.T. Arnsten *

Dept. Neuroscience, Yale Medical School, New Haven, CT, 06510, USA

ARTICLE INFO

Handling Editor: Rita Valentino

Keywords:
Norepinephrine
Stress
Prefrontal cortex
Working memory
Beta-adrenergic receptors
ADRAB1

ABSTRACT

Uncontrollable stress exposure impairs working memory and reduces the firing of dorsolateral prefrontal cortex (dlPFC) "Delay cells", involving high levels of norepinephrine and dopamine release. Previous work has focused on catecholamine actions on dlPFC pyramidal cells, but inhibitory interneurons may contribute as well. The current study combined immunohistochemistry and multi-scale microscopy with iontophoretic physiology and behavioral analyses to examine the effects of beta1-noradrenergic receptors (β1-ARs) on inhibitory neurons in layer III dlPFC. We found β1-AR robustly expressed on different classes of inhibitory neurons labeled by the calcium-binding proteins calbindin (CB), calretinin (CR), and parvalbumin (PV). Immunoelectron microscopy confirmed β1-AR expression on the plasma membrane of PV-expressing dendrites. PV interneurons can be identified as fast-spiking (FS) in physiological recordings, and thus were studied in macaques performing a working memory task. Iontophoresis of a β1-AR agonist had a mixed effect, increasing the firing of a subset and decreasing the firing of others, likely reflecting loss of firing of the entire microcircuit. This loss of overall firing likely contributes to impaired working memory during stress, as pretreatment with the selective β1-AR antagonist, nebivolol, prevented stress-induced working memory deficits. Thus, selective β1-AR antagonists may be helpful in treating stress-related disorders.

1. Introduction

Exposure to uncontrollable stress impairs the higher cognitive functions of the prefrontal cortex (PFC) in both animals and humans (Murphy et al., 1996; Roozendaal et al., 2004a; Arnsten, 2009; Liston et al., 2009; Qin et al., 2009, 2012; Rincón-Corté et al., 2019; Datta and Arnsten, 2019), contributing to risk of mental illness, including cognitive disorders such as schizophrenia and post-traumatic stress disorder (PTSD), e.g. (Mazure, 1995; Sinha, 2007; Hart et al., 2017; Holmes et al., 2019; Harnett et al., 2021; Georgiades et al., 2023). Although stress-induced PFC dysfunction may have survival value during danger when rapid, instinctive actions can be life-saving, there are multiple situations where the thoughtful functions of the PFC are needed to thrive, and to overcome mental distress (Arnsten, 2009, 2015). Thus, understanding the neural mechanisms that cause PFC dysfunction has therapeutic as well as scientific value.

Many higher cognitive functions are mediated by the dorsolateral PFC (dlPFC) in primates, including working memory, abstract reasoning, flexible decision-making, and executive functions such as planning, organization and top-down (cognitive) control of thought, action and emotion (Szczepanski and Knight, 2014). The cellular bases underlying visuospatial working memory (Funahashi et al., 1989) and top-down control (Funahashi et al., 1993) was first discovered by Goldman-Rakic (1995), who uncovered pyramidal cell microcircuits in deep layer III of dlPFC with extensive local recurrent excitation (Kritzer and Goldman-Rakic, 1995; Gonzá et al., 2000) that is needed to sustain persistent neuronal firing throughout the delay period when information is held in memory without sensory stimulation (Funahashi et al., 1989; Goldman-Rakic, 1995). These "Delay cells" are also spatially tuned, firing only for their preferred direction (Funahashi et al., 1989), where lateral inhibition from GABAergic interneurons refines the representation of visuospace held in working memory (Rao et al., 2000; González-Burgos et al., 2005). GABAergic interneurons also likely contribute to feedforward inhibition to prevent seizures in recurrent networks (Compte et al., 2000). At least some of these interneurons are fast-spiking (FS) cells, where their more narrow spikes can be detected

* Corresponding author. Dept. Neuroscience, Yale Medical School, 333 Cedar St. New Haven, CT, 06510, USA.
E-mail address: amy.arnsten@yale.edu (A.F.T. Arnsten).

https://doi.org/10.1016/j.ynstr.2024.100628
Received 16 December 2023; Received in revised form 12 March 2024; Accepted 14 March 2024
Available online 15 March 2024

with *in vivo* recordings during working memory (Rao et al., 1999; Constantinidis and Goldman-Rakic, 2002). These FS cells are likely GABAergic interneurons that express the calcium binding protein, parvalbumin (PV)(Cauli et al., 1997; Torres-Gomez et al., 2020; Rotaru et al., 2011).

A key question is how stress exposure influences these microcircuits that are so essential to working memory. Even mild acute uncontrollable stress impairs working memory, e.g. decreasing the BOLD response from the dlPFC during working memory in humans (Qin et al., 2009, 2012), and reducing Delay cell firing and impairing working memory in macaques (Murphy et al., 1996; Arnsten and Goldman-Rakic, 1998; Birnbaum et al., 2004; Vijayraghavan et al., 2007; Datta et al., 2019). These rapid changes in cognition are mediated in large part by catecholamines, with high levels of both norepinephrine (NE) and dopamine (DA) released in the PFC (Roth et al., 1988; Bradberry et al., 1991; Finlay et al., 1995), engaging low affinity α1-and β1-adrenoceptors (β1-AR) (Datta and Arnsten, 2019; Arnsten, 2015; Datta et al., 2019; Weitl and Seifert, 2008). Many of these actions occur on dendritic spines of pyramidal neurons in deep layer III, where the evidence suggests that they drive feedforward cAMP-calcium opening of K^+ channels, disconnecting recurrent excitatory microcircuits (reviewed in (Datta and Arnsten, 2019)). However, β1-AR are also known to excite PV interneurons in rodent mPFC (Luo et al., 2017), which may suppress overall PFC function. Parallel actions on interneurons in the primate dlPFC may contribute to loss of dlPFC function during stress exposure.

The current study examined this hypothesis by exploring the expression of β1-AR on PV interneurons in layer III of macaque dlPFC using both multiple label immunofluorescence (MLIF) and immunoelection microscopy (immunoEM). We also examined β1-AR expression on inhibitory neurons labeled for calbindin (CB) and calretinin (CR), which together with PV label most inhibitory neurons in primate dlPFC (Cond et al., 1994; Medalla et al., 2023). Previous research has documented β1-AR on dendritic spines of pyramidal cells in these circuits (Datta et al., 2024), but had not tested whether they were also localized on inhibitory interneurons. The physiological effects of β1-AR stimulation on PV interneurons were studied by recording from FS (presumed PV) dlPFC neurons during a visuospatial working memory task, while the clinical relevance of these findings was explored by testing whether systemic administration of a selective β1-AR antagonist could protect against stress-induced working memory deficits in monkeys.

2. Methods

All research was conducted with the approval of the Yale University IACUC under NIH and USDA guidelines.

2.1. Subjects and tissue processing for anatomy

Tissue from the dlPFC blocks of two young adult female macaques were used in this study (aged 8 and 10y). As described previously (Datta et al., 2023), subjects were deeply anesthetized and transcardially perfused with 0.1M phosphate-buffered saline (PBS), followed by 4% paraformaldehyde and 0.05% glutaraldehyde in 0.1M PBS. Brains were removed, and a dorsolateral block was sliced at 60 μm on a vibratome (Leica, Norcross GA USA). The dlPFC region analyzed is shown in Fig. 1D, and included the same area as the recording site in physiological studies. Sections were cryoprotected in increasing concentrations of sucrose solution (10, 20, 30% in PBS, each overnight), rapidly frozen in liquid nitrogen and stored long-term at −80 °C.

2.2. Primary antibodies for immunohistochemistry

To label β1-AR, we used the Alomone polyclonal rabbit anti-β1-AR at 1:100 (Alomone, cat# AAR-023, RRID:AB_2340886), which has been previously used in macaque PFC (Lee et al., 2020). We have previously shown that co-incubation with the Alomone β1-AR antigen blocking peptide (Alomone, cat# BLP-AR023) produces negligible labeling (Datta et al., 2024). To label the calcium binding proteins, we used Swant mouse monocolonal antibodies for PV, CB, and CR at 1:2000 (cat# 235 RRID:AB_10000343, cat# 300 RRID:AB_10000347, and cat# 6B3 RRID: AB_10000320, respectively), which have been widely validated (e.g. (Joyce et al., 2020)).

2.3. Multiple label immunofluorescence

2.3.1. Immunohistochemistry

Sections were selected along the mid to posterior aspect of the principal sulcus in the dlPFC (see Fig. 1D). Free-floating sections were used to label β1-AR and the calcium-binding proteins PV, CB, and CR for confocal and electron microscopy. These label most inhibitory neurons in primate cortex and are largely non-overlapping (Cond et al., 1994; Medalla et al., 2023; Joyce et al., 2020; DeFelipe, 1997). Sections underwent antigen retrieval in 10 mM sodium citrate (J.T. Baker cat# 3646-01) at 75–80 °C for 30 min, and then were cooled for another 30 min. Subsequently, they underwent a 50 mM glycine in PBS incubation for 1 h (Sigma, cat# G-7126), followed by blocking with 5% bovine serum albumin (BSA, Jackson ImmunoResearch, cat# 001-000-162), 10% normal goat serum (NGS, Jackson ImmunoResearch cat# 005-000-121), and 0.4% Triton X-100 in 0.1M phosphate buffer (PB) for 1 h. Sections were incubated in primary antibodies for 72h at 4 °C in a dilution buffer (2% BSA, 0.4% Triton X-100, 1% normal goat serum). Sections then underwent a species-specific fluorophore-conjugated goat secondary antibody incubation at 1:100 in dilution buffer for 3 h at 4 °C, in the dark (goat anti-rabbit AF488, Invitrogen cat# A11008, and goat anti-mouse AF647 Invitrogen cat# A32728). Sections were mounted using ProLong Gold Antifade Mountant (Invitrogen, cat# P36930).

2.3.2. Imaging and analysis

Sections were imaged using a Zeiss LSM 880 Airyscan with the Plan-Apochromat 20x/0.8 M27 objective. Z-stacks were obtained with ~0.3-μm steps under laser excitation at 488 nm or 633 nm. Emission filter bandwidths and sequential scanning acquisition were set up in order to avoid possible spectral overlap between fluorophores. Confocal images were deconvoluted with Hugyens Professional version 22.04 (Scientific Volume Imaging, The Netherlands, http://svi.nl). For quantitative analysis, we systematically sampled from deep layer III in two sections per case, obtaining a stack in deep layer III in every other field of view in parallel with the pial surface. The analyses focused on layer III, as this is the site of the microcircuits most linked to the generation of persistent firing needed for working memory (Goldman-Rakic, 1995). Deep layer III was identified by first examining the laminar organization of β1-AR pyramidal-like neurons from the pia to the white matter at lower magnification, and then locating layer deep III for higher magnification sampling. β1-AR pyramidal-like neurons were robustly labeled in all layers, and plentiful and large directly above the granular layer IV. The calcium binding protein label often aided in the identification of layers. For example, in dlPFC, darkly labeled CB + putative inhibitory neurons are densest in layers II-IIIa, and lightly labeled CB + putative pyramidal neurons are densest in layer IIIb. PV + neurons are sparser in layers I-II but increase in density near layer IV, while CR + neurons are densest in layers I-III (Cond et al., 1994; Joyce et al., 2020). From each stack, we extracted a single focal plane near the top or bottom of the section, where antibody penetration was optimal, ensuring that no cells were sampled twice. Then, for each image, we isolated the calcium binding protein channel for each stack (PV, CB, or CR), and traced the neuronal somata. We applied the traces to the isolated β1-AR channel, and measured the mean grey value (MGV) in the traced inhibitory neuron somata, in 3–10 "neuropil" regions with no distinguishable labeled cellular processes, and in 3–10 strongly labeled pyramidal-like β1-AR neurons. We binned the inhibitory neuron somata into categories based on their MGV in relation to the neuropil and pyramidal MGV. β1-AR negative inhibitory neuron somata had a MGV less than the average

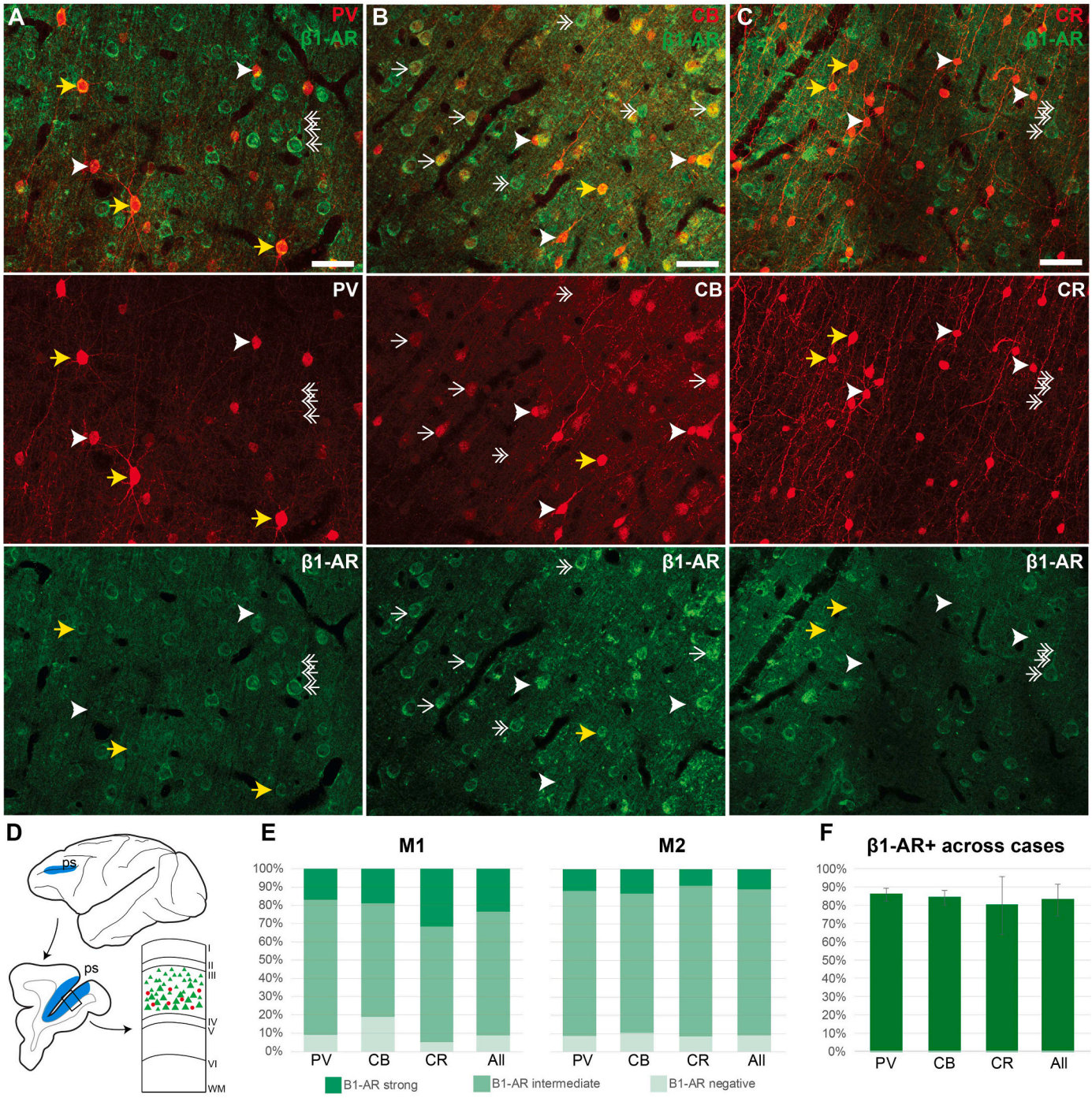

Fig. 1. β1-AR expression across inhibitory neuron types in layer III dlPFC

Maximum projections of confocal microscopy photomicrographs depicting multiple label immunofluorescence (MLIF) in deep layer III dlPFC in a young macaque (8 years), depicting β1-AR with parvalbumin (PV) **(A)**, calbindin (CB) **(B)**, or calretinin (CR) **(C)**. Yellow arrow, neuron double labeled for β1-AR (green), and PV, CB or CR (red). White arrowhead, neuron positive for PV, CB, or CR only. White double-headed arrow, pyramidal-like neuron positive for β1-AR and negative for PV, CB, or CR. White single-headed arrow, pyramidal-like neuron positive for β1-AR and lightly labeled by CB. **(D)** Schematic depicting exemplar sampling site (blue) in the mid to posterior principal sulcus (ps) of the dlPFC. Top, lateral surface of a macaque brain. Left, example coronal slice with sampling region along the principal sulcus (blue). Right, schematic of a cortical column depicting layer III, the region sampled for quantitative analysis. **(E)** Percent of PV, CB, or CR neurons that are β1-AR negative (light green, expression lower than sampled "neuropil" regions), β1-AR intermediate (intermediate green, expression above sampled "neuropil" regions, but less than expression observed in pyramidal-like neurons), or β1-AR strong (expression greater than β1-AR pyramidal-like neurons), sampled from two young monkeys (M1, 8 years, left; M2, 10 years, right). **(F)** Total β1-AR + neurons (β1-AR strong + β1-AR intermediate), averaged across M1 and M2, shown with standard deviation. In monkey 1 (M1), we analyzed 90 CB cells, 251 CR cells, and 250 PV cells. In monkey 2 (M2), we analyzed 136 CB cells, 211 CR cells, and 250 PV cells. Scale bars, 50 μm. (For interpretation of the references to color in this figure legend, the reader is referred to the Web version of this article.)

MGV across sampled neuropil, β1-AR strong inhibitory neurons had a MGV greater than the average MGV sampled across strongly labeled pyramidal-like neurons, and β1-AR intermediate inhibitory neuron somata had a MGV between the average MGV in the neuropil and the strongly labeled pyramidal-like cells. In monkey 1 (M1), we analyzed 90 CB cells, 251 CR cells, and 250 PV cells. In monkey 2 (M2), we analyzed 136 CB cells, 211 CR cells, and 250 PV cells. CB cells are most dense in layer II-IIIa, and less frequent in other layers, while CR and PV neurons are plentiful in deep layer III, in line with previous reports of density across the cortical column (Condé et al., 1994; Medalla et al., 2023). Statistics were carried out in Prism 9 (Graphpad Software, San Diego CA). Quantitative analysis, and processing of confocal Z-stacks into maximum intensity Z-projections for figures was performed using Fiji (Schindelin et al., 2012). Images were adjusted for brightness and contrast, labeled, and assembled using Adobe Photoshop CS5 Extended (version 12.0.4 × 64, Adobe Systems Incorporated) and Adobe Illustrator 25.0.1 (Adobe Systems Incorporated version 27.7).

2.4. ImmunoEM

2.4.1. Single-label immunoEM

Single-label immunogold EM was accomplished using gold-conjugated secondary antibodies paired with silver enhancement, or biotinylated secondary antibodies paired with nickel-intensified diaminobenzidine (Ni-DAB). Sections underwent a modified lower-temperature sodium citrate antigen retrieval, as above, but at 30–35 °C for 15 min, followed by a 15 min cooling period. Then, sections were incubated in glycine, as above, and blocking (5% BSA, 10% NGS, 0.4% Triton X-100, and for immunogold, 0.1% Aurion acetylated bovine serum albumin, or BSA-c, Electron Microscopy Sciences, cat# 25557). Sections were incubated for 72 h at 4 °C in the rabbit primary antibody for β1-AR at 1:100 in antibody dilution buffer (1% BSA; 1% NGS; 0.1% BSA-c; and for immunogold, 0.1% Aurion coldwater fish gelatin, CWFG Electron Microscopy Sciences cat# 25560). Species-specific secondary antibodies were utilized for both types of visualization methods. For immunogold, sections were incubated in Aurion F(ab) fragment of goat anti-rabbit ultrasmall at 1:50 (Electron Microscopy Sciences, cat#25361) at 4 °C overnight. For immunoperoxidase Ni-DAB, sections were incubated in a $F(ab')_2$ fragment biotinylated goat anti-rabbit secondary antibody at 1:200 (Jackson ImmunoResearch, cat# 111-066-003, RRID: AB_2337966) at 4 °C overnight. The following day, after washes, immunogold sections underwent a 4% paraformaldehyde (in PBS) postfix for 5 min, followed by a 10 min 50 mM glycine incubation, and then a few quick distilled water washes. Silver enhancement was performed with the Nanoprobes HQ Silver kit (cat# 2012-45 ML) in the dark for 20–30 min, and produced variable sized particles. Immunoperoxidase Ni-DAB sections were incubated in avidin-biotin complex (ABC, Vector cat# PK-6100) for 1.5 h, and then visualized using 0.025% Ni-intensified 3,3-diaminobenzidine tetrahydrochloride (Sigma Aldrich) as a chromogen in 0.1M PB with the addition of 0.005% hydrogen peroxide for about 10 min.

For the immunogold sections, we ran a tandem control section with the primary antibody omitted to test the non-specific labeling of the secondary antibody. When imaged, gold particles were extremely sparse in the test section, suggesting that the secondary antibody with silver enhancement had good specificity for the primary antibody in our sections. Previous controls in the lab have validated the specificity of the biotinylated secondary antibodies used for immunoperoxidase labeling.

2.4.2. Double-label immunoEM-

Double-label immunoEM was accomplished by pairing gold (for β1-AR) and diaminobenzidine (DAB, without nickel intensification) immunoperoxidase (for PV). Sections underwent the modified sodium citrate antigen retrieval and glycine incubations as described in the previous section. Then, sections underwent a 30 min 0.3% hydrogen peroxide incubation at 4 °C and avidin-biotin blocking (Vector cat# SP-2001) to prevent non-specific labeling by the immunoperoxidase product. Sections were then preblocked and incubated with the mouse monoclonal PV primary at 1:2000 for 48 h at 4 °C. They were incubated with biotinylated goat anti-mouse (Jackson ImmunoResearch cat# 115-066-146) at 1:200 for 3 h at room temperature, then ABC for 1.5 h, and visualized using a DAB kit (Vector cat# SK-4100, nickel excluded). Then sections were washed with PB, and incubated in the rabbit primary antibody for β1-AR at 1:100 for 48 h at 4 °C. Subsequent steps for post-fixing and silver enhancement were performed as described in the previous section. This process was performed in tandem with a paired protocol that reversed the order of the antigen labeling, first performing gold β1-AR, and then the PV DAB second, and both were imaged, demonstrating similar labeling patterns.

2.4.3. EM processing

After immunolabeling, sections underwent EM processing. Sections were first post-fixed in 4% paraformaldehyde in 0.1M PBS for 20 min. Sections were submersed in 1% osmium tetroxide in PB, followed by immediate dilution by half (to 0.5%), and the sections were incubated in the dark for 30 min at 4 °C. Then, following PB washes, sections were washed in short ascending 50% and 70% ethanol washes, before being incubated in 1% uranyl acetate in 70% ethanol for 40 min. Sections were washed in 95% and 100% ethanols, propylene oxide (Electron Microscopy Sciences cat#20401), then infiltrated with Durcupan resin (Electron Microscopy Sciences cat#14040), and baked at 60 °C for 72 h.

2.4.4. Imaging and sampling

Two sections were processed per animal, and at least two blocks of tissue from layer III of each subject were dissected from each section. Blocks were cut, and the first sections containing tissue were collected in 50 nm sections using an ultramicrotome (Leica) in several short series (up to 20 sections) on Butvar-coated (Electron Microscopy Sciences, cat #11860) copper slot grids. Grids were counterstained using 3% lead citrate (Leica Ultrostain 2, cat# 512-26-5), and imaged using a Talos L120C transmission electron microscope (Thermo Fisher Scientific). We performed an exhaustive meanderscan search approach in the region of antibody penetration for one-to-two sections per series, and searched for β1-AR + high-likelihood inhibitory dendrites (for the single-lable immunoEM) or PV+/β1-AR+ (for double-label immunoEM) labeled dendrites. Neuronal processes were identified using classical criteria (Peters et al., 1991). Briefly, inhibitory dendrites in primate cortex are aspiny or sparsely spiny, containing mitochondria, and receive frequent synapses on the dendritic shaft. In our single-label immunoEM preparation, we identified "high-likelihood" inhibitory dendrites by their lack of spines in plane (and in neighboring serial sections if needed), and by the presence of multiple asymmetric synapses in plane on a dendritic shaft. A Ceta CMOS camera was used for image capture at a range of magnifications, as needed. Images were adjusted for brightness and contrast using Adobe Photoshop, and figures were assembled in Adobe Illustrator (described above).

2.5. Physiological recordings

The oculomotor delayed response visuospatial working memory task (ODR), the iontophoretic electrode, the recording site in dlPFC, and the firing patterns of a representative Delay cell, can all be seen in Fig. 4A–D. Briefly, one rhesus monkey (*Macaca mulatta;* 15 years old, male) was trained on the ODR task, where the monkey fixates on a central point for 0.5sec to initiate a trial; a cue then comes on for 0.5sec in one of eight locations. The monkey must remember the spatial location over a delay period of 2.5sec while maintaining fixation centrally. At the end of the delay, the fixation point is extinguished, and the monkey can move its eyes to the remembered location within 1sec for juice reward. Iontophoretic, single unit recordings are made from the dlPFC subregion near the caudal principal sulcus, anterior to the frontal eye fields. This subregion of the dlPFC is known to be essential for the accurate

performance of this task, as temporary lesions to this area markedly impair performance (Chafee and Goldman-Rakic, 2000). The iontophoretic electrode contains a central carbon fiber for neuronal recording, surrounded by 6 glass micropipettes for ejection of drug solutions using minute amounts of electric current (+10–60 nA). Note that drugs must contain an electric charge to be amenable to this technique.

Recorded cells were classified into regular spiking or fast spiking neurons based on their waveforms (Fig. 4C). The waveform features, such as trough-peak ratio, trough-peak duration and end-slope at 0.27ms after trough, were used for classification (Roussy et al., 2021). Typically, regular spiking cells show long trough-peak duration and negative end-slope, while fast-spiking cells with short trough-peak duration and positive end-slope. Only Delay cells were selected for subsequent drug testing. Delay cells show persistent firing across the delay period if a cue had been presented at its "preferred direction", e.g. 180°, but not other, "nonpreferred" directions. This spatially tuned, persistent firing generates a mental representation of visual space that is foundational to visuospatial working memory. For the sake of space, figures only show the neuronal firing for a neuron's preferred direction and just one nonpreferred direction in the opposing direction. The spatial tuning of a Delay cell was analyzed using a d' measure of spatial selectivity during the delay epoch [$d' = mean_{pref}\text{-}mean_{nonpref}/\sqrt{(sd^2_{pref} + sd^2)_{nonpref}}$]. The β1-AR agonist xamoterol (Tocris Bioscience) was dissolved at 0.01 M concentration in sterile water. Data were analyzed by repeated measures analyses of variance, using two-way ANOVA with Sidak's multiple comparisons to assess the effects of drug application on the task-related activity of each Delay cell. Repeated measures two-way ANOVA with Sidak's multiple comparisons and t-tailed paired *t*-test were employed to assess the effects of drug application on task-related activity for the population analysis.

2.6. Behavior

Rhesus macaques (n = 7, 1 female, ages 9–23 years) were used in the behavioral research. Monkeys were pair-housed with daily environmental enrichment, and were food regulated (i.e. fed after cognitive testing) but not food deprived, and received daily fruits and vegetables. There were multiple daily evaluations by veterinary and animal care staff. Note that our goal is to have the monkeys as relaxed and non-stressed under vehicle conditions such that even the effects of a mild stressor on cognition can be detected. The monkeys had all been used in previous acute pharmacological experiments, including examination of adrenergic compounds, but with washout periods ≥10 days sufficient to establish a return to stable baseline cognitive performance.

The monkeys in this study had been pretrained on the delayed response task in a Wisconsin General Test Apparatus, the classic test of spatial working memory that relies on dlPFC function in monkeys (Jacobsen, 1936). In this task, the monkey watches as the experimenter bait one of two wells with a food reward, the wells are then covered with identical plaques and a screen is lowered for a prescribed delay. After the delay period is over, the screen is raised and the monkey must choose based on its memory of the location of the baited well. The spatial position of the reward randomly changes over the 30 trials that make up a daily test session, and the monkey must constantly update the contents of working memory to perform correctly. In this study, variable delays were used, ranging from 0 s to the delay that produced chance performance, and were adjusted to produce overall baseline performance of ~70% correct, thus leaving room for either improvement or impairment in performance. The monkeys were tested twice a week, by an experimenter who was blind to drug treatment conditions but highly familiar with the normative behavior of each monkey. In addition to performance on the task, they were rated for potential changes in sedation, agitation or aggression using rating scales. For sedation/agitation, a score of 4 was too sedated to test, 3 marked sedation, 2 moderate sedation, 1 quieter than usual, 0 normal, −1 more alert than usual, −2 more agitated than usual, −3 marked agitation, −4 too agitated to test. For aggression ratings, a score of 0 was normal, −1 was slightly more aggressive than usual, −2 more aggressive than usual, −3 marked aggression, −4 too aggressive to test safely. For monkeys that are naturally aggressive, scores of 1 or 2 were used to indicate less aggressive than usual.

Stress research in monkeys is challenging, as we need to use mild stressors, for ethical reasons, and so that the animal will perform all trials. Our early studies found that loud noise (>95 dB) –a stressor used in human studies (Hockey, 1970; Glass et al., 1971; Hartley and Adams, 1974)– impaired accuracy, but the monkeys rapidly habituated to this stressor, which was problematic for drug challenges (Arnsten and Goldman-Rakic, 1998). We found that we could mimic the effects of noise stress by using the benzodiazepine inverse agonist, FG7142 (Murphy et al., 1996; Birnbaum et al., 2004), which produces a classic physiological stress response in humans, monkeys and rats, including NE release in PFC (Nakane et al., 1994; Dazzi et al., 2002) and cortisol release (Dorow et al., 1983; Ninan et al., 1982; File et al., 1985; Pellow and File, 1986; Takamatsu et al., 2003; Sevastre-Berghian et al., 2018), and discriminates similar to footshock in rats (Leidenheimer and Schechter, 1988). FG7142 allows us to optimize the dose for each animal and produce consistent effects; we have used this compound for almost 30 years with reliable results. Please note that FG7142 impairs accuracy on tasks requiring PFC cognitive tasks, but does not impair performance of control tasks with similar motor and motivational demands that do not depend on the PFC (Murphy et al., 1996; Arnsten and Goldman-Rakic, 1998).

Nebivolol (Tocris Bioscience) was diluted in a combination of 0.2 mls ETOH and 0.8 mls sterile water and given p.o. in a small piece of cereal bar 1 h before testing. FG7142 (Tocris Bioscience) was suspended in a vehicle of 0.2 mls DMSO and 0.8 mls HBC (2-Hydroxypropyl-*β*-cyclodextrin, Tocris Bioscience) immediately prior to use and was injected i.m. 30 min prior to cognitive testing. There was at least a 10-day washout period between doses, with monkeys required to return to stable baseline performance prior to subsequent drug treatment. Following initial tests to determine the effective dose of FG7142 for each monkey, and the proper range for nebivolol challenge, the subsequent order of drug administration was semi-random between animals to minimize order effects. All drug effects were compared to vehicle control, with statistical analyses using paired (within subjects) two-tailed T-tests with p = 0.05 as the level of significance.

3. Results

3.1. Multiple label immunofluorescence

The expression of β1-AR in inhibitory neurons labeled for PV, CB or CR in deep layer III of dlPFC was examined using multiple label immunofluorescence. Double-label immunofluorescence of β1-AR with PV, CB, or CR in layer deep III demonstrated that PV, CB, and CR neurons can be positive or negative for β1-AR (Fig. 1A–C, yellow arrows and white arrowheads, respectively). The strongest labeling appeared in pyramidal-like neurons, with large pyramidal-shaped somata and apical dendrites oriented toward the pia (Fig. 1A–C, double-headed white arrows), consistent with our previous data demonstrating β1-AR in layer III pyramidal cells (Datta et al., 2024). Nuclear labeling for β1-AR appeared largely absent across all cell types.

To quantify the expression of β1-AR across interneuron subtypes, we systematically sampled deep layer III (Fig. 1D) in two sections per case, and extracted single focal planes from the top and bottom of each stack for β1-AR expression analysis. For each focal plane, we traced the PV, CB, or CR somata and measured the β1-AR mean grey value (MGV) in each soma. Within each image, we then compared that to i) the average MGV across sampled "neuropil" regions with no β1-AR immunopositive neuronal processes (excluding blood vessels), and ii) the average MGV in strongly labeled pyramidal-like somata in plane in areas of equivalent and consistent illumination. Thus, data from each focal plane was

normalized for combining across stacks, sections and cases. Results from our quantitative analysis are shown in Fig. 1E–F. In both cases, most PV, CB, or CR neurons were positive for β1-AR. The first monkey (M1, 8 years) had more cells negative for β1-AR, meaning the expression within the cell was below that of nearby immunonegative neuropil regions, particularly for CB interneurons. Both animals contained at least 10% of neurons that had β1-AR expression equivalent to strongly labeled, nearby pyramidal-like neurons. Combined data across cases demonstrated that ~80% of PV, CB, and CR cases sampled from deep layer III dlPFC were positive for β1-AR, and there were no statistically significant differences across inhibitory neuron subtypes.

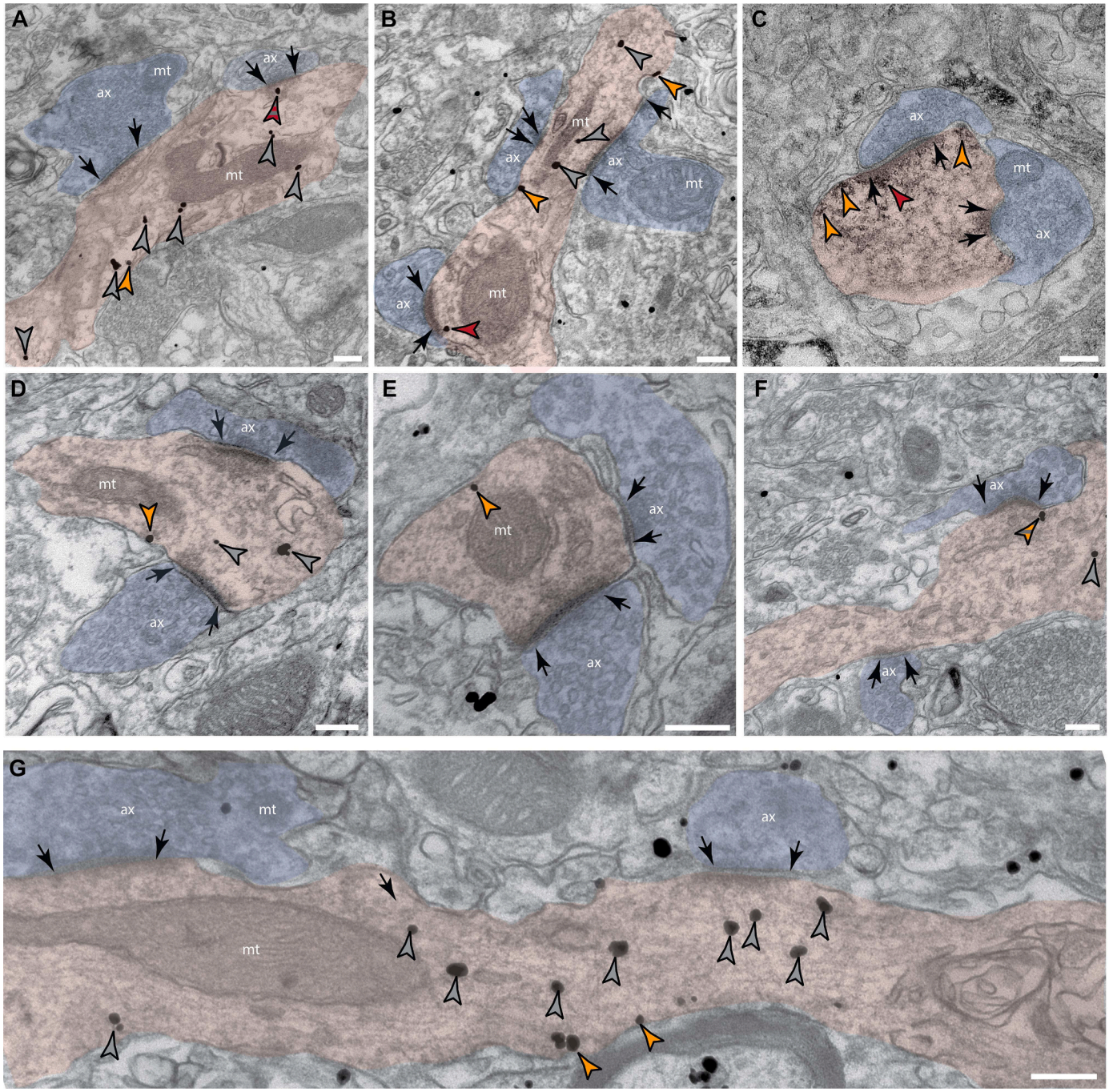

Fig. 2. β1-AR expression in high-likelihood inhibitory dendrites of layer III dlPFC
(A-G) Electron microscopy photomicrographs depicting β1-AR expression in high-likelihood inhibitory dendrites (pseudocolored pink) of young macaque layer III dlPFC (8-10y). Dendrites were classified as high-likelihood inhibitory based on multiple criteria, including multiple asymmetric synapses (presumed excitatory, black arrows) on the dendritic shaft, and no apparent spines in plane or in nearby sections. β1-AR immunogold [or immunoperoxidase nickel DAB (C)] labeling (arrowheads) indicate the presence of β1-AR expression in the cytoplasm (grey arrowheads), in extrasynaptic segments of the membrane (orange arrowheads), or in or near the post-synaptic density (red arrowheads). Label that appeared very close to a membrane but not clearly adhered was color coded with hatching to capture that they may be undergoing trafficking to a specific membrane compartment. Red/grey hatching captures possible trafficking to the synapse, and orange/grey hatching captures possible trafficking to an extrasynaptic location. ax, axon (pseudocolored blue); mt, mitochondria. Scale bars, 200 nm. (For interpretation of the references to color in this figure legend, the reader is referred to the Web version of this article.)

3.2. Immunoelectron microscopy

ImmunoEM was utilized to examine β1-AR expression within dendrites of inhibitory neuronal processes in layer III of dlPFC. Fig. 2 demonstrates that high likelihood inhibitory dendrites, i.e. classified by lack of spines and multiple asymmetric synapses on the dendritic shaft, contain β1-AR at cytoplasmic locations (Fig. 2A–B,D,F-G, grey arrowheads, likely intracellular trafficking), at extrasynaptic locations

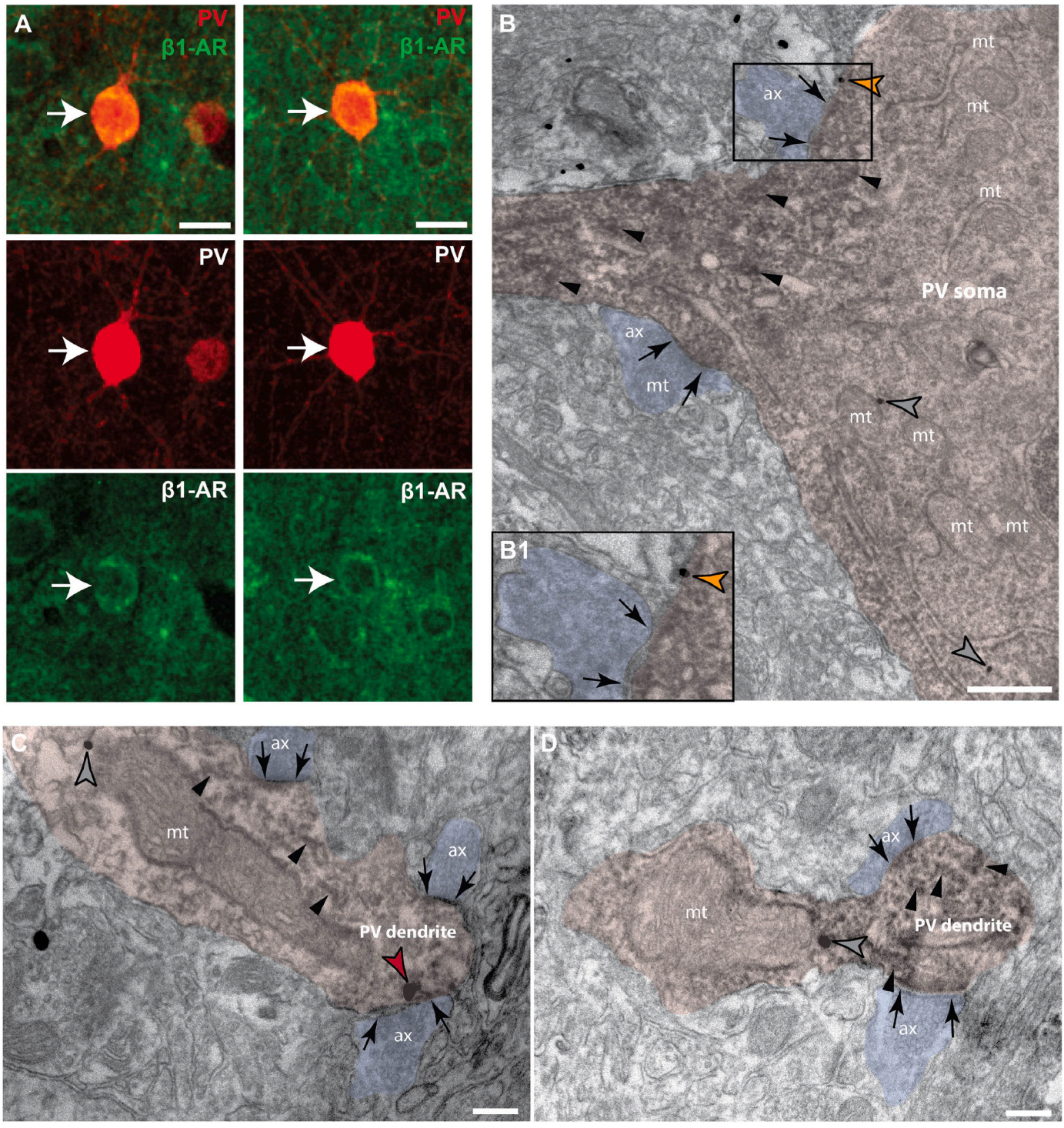

Fig. 3. β1-AR expression in PV neurons of layer III dlPFC
(A) Confocal microscopy photomicrographs of deep layer III dlPFC parvalbumin (PV) neurons (red) with robust β1-AR expression (green) in the cytoplasm of the somata. Scale bars, 15 μm **(B)** Electron microscopy photomicrograph of a PV soma and proximal dendritic segment (pseudocolored pink), labeled with the immunoperoxidase DAB (dark precipitate, black arrowheads). Cytoplasmic (grey arrowheads) and extrasynaptic β1-AR (orange arrowhead) are labeled with immunogold (dark quantal structures). The soma and proximal segment receive asymmetric (presumably excitatory) synapses (black arrows) from axons (pseudocolored blue). Scale bar, 500 nm. **(C)** PV dendrite expressing β1-AR (labeled by DAB, black arrowheads), receiving multiple asymmetric synapses on the dendritic shaft, featuring synaptic β1-AR expression (red arrowhead). (D) PV dendrite expressing cytoplasmic β1-AR (grey arrowhead). ax, axon; mt, mitochondria. Scale bars for C-D, 200 nm. (For interpretation of the references to color in this figure legend, the reader is referred to the Web version of this article.)

(Fig. 2A–G, orange arrowheads), and in or near the post-synaptic density of asymmetric synapses (Fig. 2A–C). These dendrites could be positive for PV, CB, or CR.

Given that the FS neurons are critical for shaping the tuning properties of deep layer III dlPFC neuronal assemblies subserving cognition, we then examined PV neurons specifically (Fig. 3). Using double-label immunoEM, we demonstrated β1-AR labeling in PV + inhibitory neuron processes in layer III dlPFC. In a PV + cell soma and proximal dendritic segment, cytoplasmic and extrasynaptic β1-AR labeling is present (Fig. 3B). PV + dendritic segments also express β1-AR synaptically (Fig. 3C) and in the cytoplasm (Fig. 3D). Thus the PV neurons, which are putatively FS, express β1-AR specifically.

3.3. Preliminary physiological data

Please note that these physiological results should be considered preliminary given the small numbers of FS neurons captured; however, the data were included due to their potential relevance to the anatomical findings described above. The current study recorded single units from the dlPFC surrounding the caudal principal sulcus, coupled with iontophoresis, in macaques performing the oculomotor delayed response test of visuospatial working memory (Fig. 4A–B). The waveforms were analyzed to distinguish the subset of FS neurons from RS cells (Fig. 4C), focusing on those with delay-related firing (Fig. 4D). Regular-spiking (RS) cells predominate in primate dlPFC, and thus recordings of FS neurons are relatively rare. Only small numbers of FS neurons were found, but considered potentially helpful to the current study and thus are included here.

The current study was able to capture 7 FS neurons during iontophoresis of the selective β1-AR agonist, xamoterol. Previous research has shown that this β1-AR agonist greatly reduces the firing of RS cells (Datta et al., 2024), e.g. as seen in Fig. 4E–G, where 11 RS cells reduced their firing following iontophoresis of xamoterol (**F**, delay firing: R-two-way ANOVA, $F_{directionxdrug}(1, 10) = 13.448$, $p = 0.0043$; Sidak's multiple comparisons: preferred direction, $p < 0.0389$ and non-preferred direction, $p = 0.7599$; G, paired *t*-test, n = 11, P = 0.000591). The current study found that 5 FS were also depressed by β1-AR stimulation (Fig. 4H–J; I, delay firing: R-two-way ANOVA, $F_{directionxdrug}(1, 4) = 27.696$, $p = 0.0062$; Sidak's multiple comparisons: preferred direction, $p < 0.0342$ and non-preferred direction, $p = 0.33$; J, paired *t*-test, P = 0.0363). As the activity of FS cells (presumed PV interneurons) is thought to be driven by pyramidal cells, and the iontophoresis of the β1-AR agonist likely influences an entire local microcircuit, these results are consistent with the loss of firing of pyramidal cells following β1-AR agonist administration leading to a loss of drive on FS interneurons. However, 2 FS cells showed increased firing

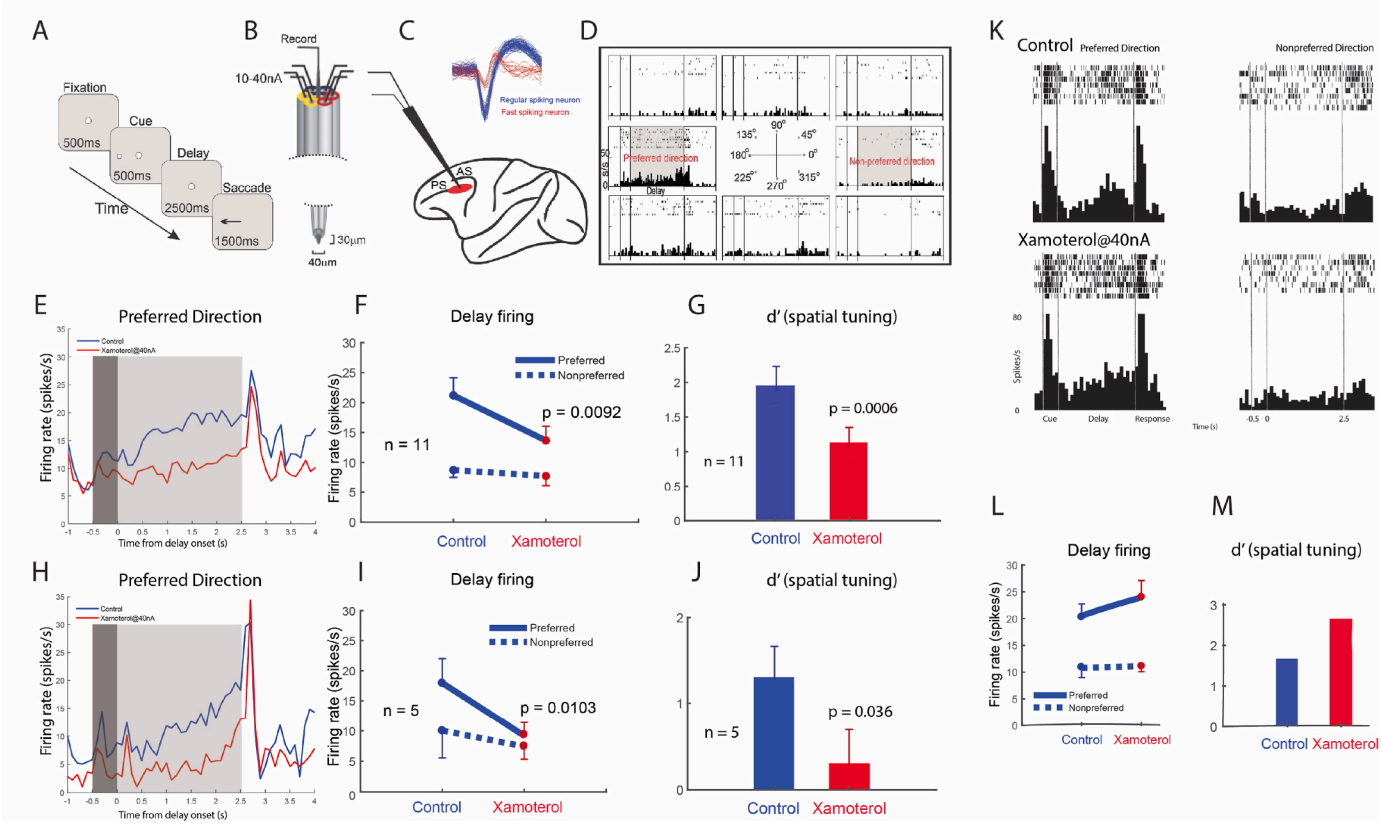

Fig. 4. Preliminary data showing that β1-AR stimulation increases the firing of a small subset of FS neurons and reduces the firing of RS neurons in dlPFC
(A) The ODR working memory task, **(B)** The iontophoretic electrode: a carbon fiber and surrounding glass micropipettes for drug delivery, with a tip diameter of around 40 µm. **(C)** The dlPFC recording site (PS = principal sulcus; AS = arcuate sulcus). The insert shows waveforms of regular spiking (RS) and fast spiking (FS) neurons. **(D)** An example of a regular spiking Delay cell, with sustained delay-related firing for its preferred direction only. **(E-G)** show that xamoterol decreased the firing of regular spiking neurons (n = 11), reducing firing rate (**E**, **F**, delay firing: R-two-way ANOVA, $F_{directionxdrug}(1, 10) = 13.448$, $p = 0.0043$; Sidak's multiple comparisons: preferred direction, $p < 0.0389$ and non-preferred direction, $p = 0.7599$) and spatial tuning (**G**, paired *t*-test, n = 11, P = 0.000591). The dark grey area, Cue epoch; light grey area, Delay epoch. **(H-J)** show that xamoterol also reduced the firing rate of most fast spiking neurons, reducing both firing rate (**H**, **I** delay firing: R-two-way ANOVA, $F_{directionxdrug}(1, 4) = 27.696$, $p = 0.0062$; Sidak's multiple comparisons: preferred direction, $p < 0.0342$ and non-preferred direction, $p = 0.33$) and spatial tuning (**J**, paired *t*-test, P = 0.0363). **(K-M)** A single cell example of a fast spiking neuron that showed increased firing with xamoterol, showing that both its delay-related firing (**K**, **L**, control vs. xamoterol@40 nA condition: two-way ANOVA, $F_{directionxdrug}(1,13) = 1.58$, $p = 0.2555$; $F_{drug}(1,13) = 8.499$, $p = 0.0268$; $F_{direction}(1,13) = 17.39$, $p = 0.0059$; Sidak's multiple comparisons: preferred direction, $p = 0.0163$ and non-preferred direction, $p = 0.73$), and spatial tuning (**M**) were increased by xamoterol. The neuron did not return to control levels of firing after xamoterol was washed out, suggesting potential second messenger actions.

with application of the β1-AR agonist xamoterol (one example shown in Fig. 4K-M; L, control vs. xamoterol@40 nA condition: two-way ANOVA, $F_{directionxdrug}(1,13) = 1.58$, $p = 0.2555$; $F_{drug}(1,13) = 8.499$, $p = 0.0268$; $F_{direction}$ $(1,13) = 17.39$, $p = 0.0059$; Sidak's multiple comparisons: preferred direction, $p = 0.0163$ and non-preferred direction, $p = 0.73$), consistent with *in vitro* recordings from rodent mPFC (Luo et al., 2017).

3.4. Cognitive performance

The current study examined whether pretreatment with the selective β1-AR antagonist, nebivolol, would protect working memory from the detrimental effects of the pharmacological stressor, FG7142 (see Methods for detailed explanation of why this stressor was selected for this research).

We first examined the effects of nebivolol (0.01–1.0 mg/kg, po, 1 h before testing) on its own, and found that the highest dose (1.0 mg/kg) significantly improved performance of the delayed response task compared to vehicle control (Fig. 5A; n = 5, p < 0.02, n = 5). There was no evidence of side effects (sedation and aggression scores were all the same as vehicle control).

We next tested whether lower doses of nebivolol that had no effect on their own would protect working memory from the detrimental effects of stress. As shown in Fig. 5B–C, pretreatment with either 0.01 mg/kg or 0.1 mg/kg nebivolol prevented the impairment in delayed response performance caused by FG7142 (0.01 mg/kg nebivolol experiment, n = 5: vehicle + FG7142 vs. vehicle + vehicle: p = 0.004; 0.01 mg/kg + FG7142: p = 0.023 compared to FG7142+vehicle; 0.1 mg/kg nebivolol experiment, n = 5: vehicle + FG7142 vs. vehicle + vehicle: p = 0.001; 0.1 mg/kg + FG7142: p = 0.002 compared to FG7142+vehicle). FG7142 produced errors at all delay lengths, and these were normalized by nebivolol. Errors following the "0" sec delay are consistent with dlPFC function needed to overcome the distraction of the screen going down and then rapidly raised during this condition. Thus, blockade of β1-AR with nebivolol was effective in preventing the cognitive deficits produced by the pharmacological stressor.

4. Discussion

4.1. Summary and evaluation of findings

The current study found that, in addition to their extensive expression on dendritic spines of pyramidal neurons (Datta et al., 2024), β1-AR are also localized on interneurons in layer III dlPFC, including ultrastructural evidence of β1-AR on the plasma membranes of PV-expressing dendrites. β1-AR were seen on all three subgroups of interneurons, i.e. those expressing PV, CB or CR. It is noteworthy that the expression patterns of β1-AR on interneurons in the macaque dlPFC were largely similar to those found in mouse mPFC (Liu et al., 2014), with the exception that mouse had fewer β1-ARs on CR interneurons, while the current study found generally similar expression across all interneuron subtypes.

One can attempt to translate across methods from the electron microscopic to the light microscopic level, but must maintain caution in doing so. It's likely that the immunopositive inhibitory dendrites we observed using immunoEM were processes of the large population of intermediate and strongly labeled neuronal somata we observed using immunofluorescence. However, because translation can occur in dendrites (Holt et al., 2019), away from the perisomatic region, we cannot rule out that some of the β1-AR negative somata we observed using immunofluorescence had β1-AR immunopositive dendritic labeling that could be detected using the higher resolution, and more sensitive, immunoEM methods.

Only PV interneurons can be recognized *in vivo* from their narrower action potential, and are thus known as FS neurons. Preliminary physiological recordings of FS neurons from macaques performing a visuospatial working memory task found limited evidence that β1-AR stimulation could excite a subset of these presumed PV interneurons, consistent with *in vitro* recordings from rodent mPFC (Luo et al., 2017). However, most FS interneurons, like the RS neurons, reduced their firing following β1-AR stimulation, likely reflecting the general reduction in the activity of the entire microcircuit when pyramidal cell activity is reduced. Behavioral studies showed the first evidence that systemic administration of the selective β1-AR antagonist, nebivolol, was able to protect working memory performance from the detrimental effects of stress exposure, emphasizing the importance of β1-AR mechanisms to stress-induced cognitive dysfunction.

There were several inherent weaknesses in this study. The small number of recordings of FS neurons was suboptimal and thus considered only preliminary in nature, but was due to the rarity of these neurons when recording from the dlPFC in cognitively-engaged monkeys. Given that PV interneurons rely on activation by glutamatergic pyramidal cells, and β1-AR stimulation reduces pyramidal cell firing, this loss of excitatory drive to FS neurons may have outweighed their excitation by β1-AR stimulation in many interneurons. β-AR stimulation has been

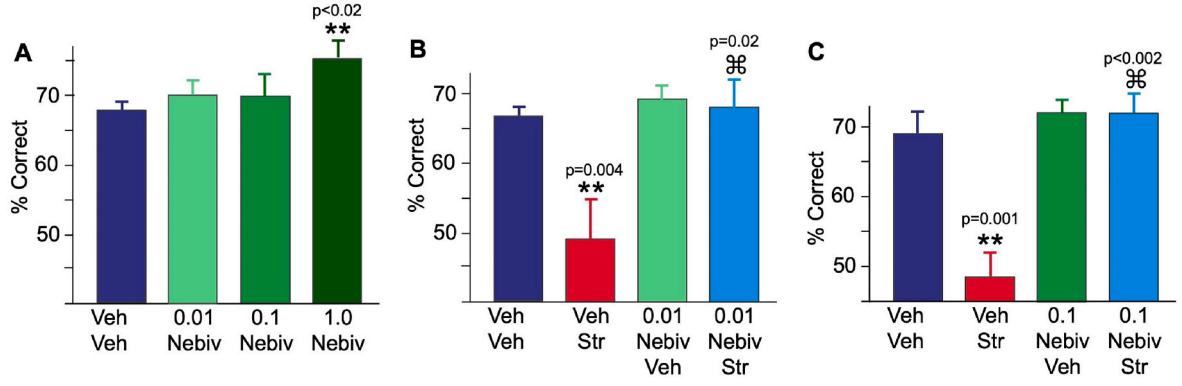

Fig. 5. Systemic administration of the β1-AR antagonist, nebivolol, protects working memory performance from stress exposure.
(A) Nebivolol on its own had no effect compared to vehicle with 0.01 mg/kg or 0.1 mg/kg, but significantly improved performance following 1.0 mg/kg. The range of scores for vehicle was 60–73% correct; for 0.01 mg/kg, 63–77% correct, for 0.1 mg/kg, 57–73% correct, and for 1.0 mg/kg, 70–80% correct. **(B)** Pretreatment with 0.01 mg/kg nebivolol, which had no effect on its own, prevented the impairment on delayed response performance caused by the pharmacological stressor, FG7142. The range of scores for vehicle + vehicle was 63–70% correct; for FG7142+vehicle, 40–57% correct, for 0.01 mg/kg nebivolol + vehicle, 63–77% correct, and for 0.01 nebivolol mg/kg + FG7142, 57–77% correct. **(C)** Pretreatment with 0.1 mg/kg nebivolol, which had no effect on its own, prevented the impairment on delayed response performance caused by the pharmacological stressor, FG7142. The range of scores for vehicle + vehicle was 63–73% correct; for FG7142+vehicle, 40–53% correct, for 0.1 mg/kg nebivolol + vehicle, 70–73% correct, and for 0.1 nebivolol mg/kg + FG7142, 67–80% correct. ** signifies different from vehicle control; ⌘ signifies different from FG7142+vehicle.

shown to excite GABA interneurons in the mouse mPFC (Luo et al., 2017), and dentate gyrus (Seo et al., 2021), but additional *in vitro* studies would be needed to reliably determine how β1-AR stimulation alters the firing of GABAergic interneuron subtypes in the primate PFC. As CB and CR interneurons cannot be reliably distinguished from pyramidal cells *in vivo*, the effects of β1-AR stimulation on these subtypes remain unknown. Another consideration is the systemic treatment in the behavioral study, where the β1-AR antagonist would act throughout the neuroaxis and not be specific to the dlPFC. However, the systemic administration is immediately relevant to potential treatment strategies (see below), and thus provides valuable data.

4.2. Working model of β1-AR actions in primate dlPFC

A working model of β1-AR actions on the microcircuits in layer III of primate dlPFC is shown in Fig. 6. In this model, high levels of NE release during stress stimulate β1-AR, reducing dlPFC Delay cell firing and impairing working memory by two complementary mechanisms: 1) The current study shows that β1-AR are commonly expressed on PV interneurons, where they may drive inhibition of pyramidal cells (Fig. 6A); and 2) Previous work has shown that β1-AR are also concentrated on pyramidal cell dendritic spines, where they weaken the efficacy of NMDAR synapses via high levels of cAMP-calcium signaling opening nearby K^+ channels (Datta et al., 2024) (Fig. 6B), e.g. similar to that seen with dopamine D1R (Gamo et al., 2015). *In vitro* slice recordings from macaque dlPFC would be needed to confirm that β1-AR stimulation excites PV (and possibly other) interneurons in macaque dlPFC, as has been seen in rodent mPFC (Luo et al., 2017). In rodent, NE activation of interneurons in orbital PFC mediates the "giving up" behaviors that can occur with chronic stress exposure (Li et al., 2023), and the current study of PV interneurons may be detecting a related mechanism in the primate dlPFC. Given that the rodent mPFC has fewer recurrent excitatory connections on spines than the highly spinous primate layer III dlPFC (Elston, 2000; Elston et al., 2011), catecholamine actions on interneurons may predominate in rodents, while β1-AR actions on spines may have an increasing role in the recently evolved primate dlPFC. Note that the potential roles of β1-AR on CB and CR interneurons are unknown.

These β1-AR actions on microcircuits in dlPFC may be involved with the rapid changes in cortical network connectivity in response to an unexpected environmental event (Bouret and Sara, 2005) or a mild stressor (Hermans et al., 2011), e.g. weakening dlPFC connectivity and strengthening those of the salience network (Hermans et al., 2011), the latter replicated with locus coeruleus activation in mice (Zerbi et al., 2019). With more sustained or aversive experiences, there is more long-lasting dlPFC dysfunction, while the amygdala is strengthened, where β1-AR play an important role in increasing amygdala's role in conditioned fear and memory consolidation of emotional events as described in more detail below (Roozendaal et al., 2004a; Cahill and McGaugh, 1996; Dę et al., 2011; Ghiasvand et al., 2011; Murchison CF et al., 2011; Luo Y et al., 2020).

4.3. Relevance to treatment of stress-related mental disorders

Given the major role of stress in exacerbating the symptoms of cognitive disorders, the current data also have relevance to the potential treatment of PFC deficits in mental illness. For example, deficits in dlPFC function are evident in schizophrenia (Weinberger et al., 1986; Glantz and Lewis, 2000; Perlstein et al., 2001; Driesen et al., 2008; Barch and Ceaser, 2012), depression (Holmes et al., 2019), bipolar disorder (Blumberg et al., 1999, 2003), PTSD (Harnett et al., 2021; Aupperle et al., 2012; Holmes et al., 2018), substance abuse (Smith et al., 2023), and Alzheimer's disease (Hof and Morrison, 1991; Schroeter et al., 2012), all of which are worsened or caused by stress exposure (Mazure, 1995; Sinha, 2007; Hart et al., 2017; Georgiades et al., 2023; Johansson et al., 2013; Nook et al., 2018). Treatment strategies for many of these disorders utilize repetitive transcranial magnetic stimulation to strengthen the left dlPFC and help restore top-down regulation e.g (George et al., 2013; Gomis-Vicent et al., 2019), and thus, pharmacological strategies that restore PFC top-down regulation may also be helpful.

Decades of research have shown that PTSD is associated with increased NE signaling (Southwick et al., 1993, 1999; Bremner et al., 1997; Pitman et al., 2012). PTSD symptoms are increased by exposure to reminders of trauma and other stressors that likely cause increased NE release (Southwick et al., 1993, 1999; Bremner et al., 1997; Pitman et al., 2012), and thus pharmacological treatments that target the NE system have been a focus for decades. The nonselective β-AR antagonist, propranolol, is currently used to treat PTSD, although with mixed results (Pitman et al., 2012; Brunet et al., 2018; Roullet et al., 2021). Propranolol has higher affinity for β2-AR than β1-AR (Baker, 2005) (log Kd for β1-AR: −8.16; β2-AR −9.08), and as stimulation of β2-AR improves working memory (Ramos et al., 2008) and protects against amygdala-driven tachycardia (Fortaleza et al., 2012), blockade of this

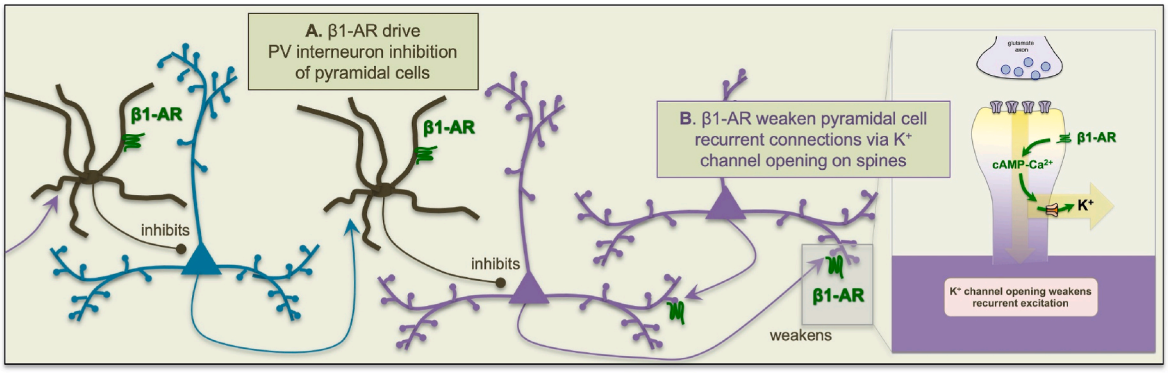

Fig. 6. Working model of β1-AR mechanisms in layer III dlPFC
We hypothesize that high levels of NE release during stress engage low affinity β1-ARs, which take dlPFC "offline" to switch control of behavior to more primitive circuits, e.g. mediated by the amygdala. The data indicate that β1-AR can reduce the firing of dlPFC Delay cells by at least two mechanisms: **(A)** The current study shows that β1-AR are expressed on GABAergic interneurons, including PV-expressing interneurons, where β1-AR drive GABAergic inhibition of pyramidal cell firing. **(B)** Our previous work has shown that β1-ARs are also highly concentrated on the dendritic spines of pyramidal cells, that weaken recurrent excitation by increasing cAMP-calcium opening of nearby K^+ channels, reducing the recurrent excitatory connections needed for working memory. As interneurons are activated by pyramidal cells as well as by β1-AR, the loss of pyramidal cell firing would ultimately reduce PV interneuron firing as well, where the entire microcircuit may have low levels of firing. Note that the roles of calretinin (CR)- and calbindin (CB)-expressing interneurons are still to be determined, but β1-AR excitation of CB-expressing interneurons would theoretically add to pyramidal cell inhibition.

receptor by propranolol may be counterproductive, and may require higher doses that are more prone to side effects. The current results suggest that a more selective, β1-AR antagonist may provide a more targeted approach, not only for protecting dlPFC function, but in the amygdala as well, which is a key site of NE actions during stress (Cahill and McGaugh, 1996; Cahill et al., 1994; Bush et al., 2010; Roozendaal and McGaugh, 2011), and where β1-AR expression is increased by fear conditioning (Fu et al., 2008). Recent research in rodent amygdala shows that the beneficial effects of β-AR blockade in reducing the conditioned fear response in the amygdala are due to β1-AR and not β2-AR (Luo Y et al., 2020). The β1-AR subtype also mediates the enhancing effects of NE on memory consolidation (Ghiasvand et al., 2011; Murchison CF et al., 2011; Roozendaal et al., 2004b), which can be problematic in the context of traumatic memories in PTSD (Cahill and McGaugh, 1996; Dę et al., 2011). Taken together with the current results, the evidence suggests that β1-AR antagonists may be superior to nonselective β-AR antagonists in treating PTSD, but further research is needed to clarify the role of β2-AR stimulation in primate PFC, and in stress-induced PFC deficits.

4.4. Conclusions

The current study found that β1-ARs are localized on GABAergic interneurons, including PV-expressing interneurons in the primate dlPFC, where their activation may contribute to the weakening of dlPFC Delay cell firing and cognitive function during stress exposure. Increased activation of PV interneurons under threatening conditions may provide a very rapid mechanism to inhibit PFC top-down control and switch behavioral control to more instinctive mechanisms. As the β1-AR also mediates the conditioned fear response in the amygdala, selective β1-AR antagonists may be more effective than propranolol in treating PTSD and related stress disorders.

Funding

This research was funded by R01 MH130538-01A1 to AFTA.

CRediT authorship contribution statement

M.K.P. Joyce: Writing – review & editing, Visualization, Resources, Methodology, Investigation, Formal analysis, Data curation, Conceptualization. **S. Yang:** Writing – review & editing, Methodology, Investigation, Formal analysis, Data curation. **K. Morin:** Writing – review & editing, Methodology, Data curation. **A. Duque:** Writing – review & editing, Methodology, Investigation. **J. Arellano:** Writing – review & editing, Methodology, Investigation. **D. Datta:** Writing – review & editing, Methodology, Investigation, Data curation. **M. Wang:** Writing – review & editing, Methodology, Investigation, Data curation, Conceptualization. **A.F.T. Arnsten:** Writing – review & editing, Writing – original draft, Supervision, Project administration, Formal analysis, Conceptualization.

Declaration of competing interest

The authors have no conflicts of interest with this study.

Data availability

Data will be made available on request.

Acknowledgements

We thank Lisa Ciavarella, Tracy Sadlon, Sam Johnson and Michelle Wilson for their invaluable contributions.

References

Arnsten, A.F.T., 2009. Stress signaling pathways that impair prefrontal cortex structure and function. Nat. Rev. Neurosci. 10, 410–422.
Arnsten, A.F., 2015. Stress weakens prefrontal networks: molecular insults to higher cognition. Nat. Neurosci. 18, 1376–1385.
Arnsten, A.F.T., Goldman-Rakic, P.S., 1998. Noise stress impairs prefrontal cortical cognitive function in monkeys: evidence for a hyperdopaminergic mechanism. Arch. Gen. Psychiatr. 55, 362–369.
Aupperle, R.L., Allard, C.B., Grimes, E.M., Simmons, A.N., Flagan, T., Behrooznia, M., Cissell, S.H., Twamley, E.W., Thorp, S.R., Norman, S.B., et al., 2012. Dorsolateral prefrontal cortex activation during emotional anticipation and neuropsychological performance in posttraumatic stress disorder. Arch. Gen. Psychiatr. 69, 360–371.
Baker, J.G., 2005. The selectivity of beta-adrenoceptor antagonists at the human beta1, beta2 and beta3 adrenoceptors. Br. J. Pharmacol. 144, 317–322.
Barch, D.M., Ceaser, A., 2012. Cognition in schizophrenia: core psychological and neural mechanisms. Trends Cognit. Sci. 16, 27–34.
Birnbaum, S.B., Yuan, P., Wang, M., Vijayraghavan, S., Bloom, A., Davis, D., Gobeske, K., Sweatt, D., Manji, H.K., Arnsten, A.F.T., 2004. Protein kinase C overactivity impairs prefrontal cortical regulation of working memory. Science 306, 882–884.
Blumberg, H.P., Stern, E., Ricketts, S., Martinez, D., de Asis, J., White, T., Epstein, J., Isenberg, N., McBride, P.A., Kemperman, I., et al., 1999. Rostral and orbital prefrontal cortex dysfunction in the manic state of bipolar disorder. Am. J. Psychiatr. 156, 1986–1988.
Blumberg, H.P., Leung, H.C., Skudlarski, P., Lacadie, C.M., Fredericks, C.A., Harris, B.C., Charney, D.S., Gore, J.C., Krystal, J.H., Peterson, B.S., 2003. A functional magnetic resonance imaging study of bipolar disorder: state- and trait-related dysfunction in ventral prefrontal cortices. Arch. Gen. Psychiatr. 60, 601–609.
Bouret, S., Sara, S.J., 2005. Network reset: a simplified overarching theory of locus coeruleus noradrenaline function. Trends Neurosci. 28, 574–582.
Bradberry, C.W., Lory, J.D., Roth, R.H., 1991. The anxiogenic beta-carboline FG 7142 selectively increases dopamine release in rat prefrontal cortex as measured by microdialysis. J. Neurochem. 56, 748752.
Bremner, J.D., Innis, R.B., Ng, C.K., Staib, L.H., Salomon, R.M., Bronen, R.A., Duncan, J., Southwick, S.M., Krystal, J.H., Rich, D., et al., 1997. Positron emission tomography measurement of cerebral metabolic correlates of yohimbine administration in combat-related posttraumatic stress disorder. Arch. Gen. Psychiatr. 54, 246–254.
Brunet, A., Saumier, D., Liu, A., Streiner, D.L., Tremblay, J., Pitman, R.K., 2018. Reduction of PTSD symptoms with pre-reactivation propranolol therapy: a randomized controlled trial. Am. J. Psychiatr. 175, 427–433.
Bush, D.E., Caparosa, E.M., Gekker, A., Ledoux, J., 2010. Beta-adrenergic receptors in the lateral nucleus of the amygdala contribute to the acquisition but not the consolidation of auditory fear conditioning. Front. Behav. Neurosci. 4, 154.
Cahill, L., McGaugh, J.L., 1996. Modulation of memory storage. Curr. Opin. Neurobiol. 6, 237–242.
Cahill, L., Prins, B., Weber, M., McGaugh, J.L., 1994. Beta-adrenergic activation and memory for emotional events. Nature 371, 702–704.
Cauli, B., Audinat, E., Lambolez, B., Angulo, M.C., Ropert, N., Tsuzuki, K., Hestrin, S., Rossier, J., 1997. Molecular and physiological diversity of cortical nonpyramidal cells. J. Neurosci. 17, 3894–3906.
Chafee, M.V., Goldman-Rakic, P.S., 2000. Inactivation of parietal and prefrontal cortex reveals interdependence of neural activity during memory-guided saccades. J. Neurophysiol. 83, 1550–1566.
Compte, A., Brunel, N., Goldman-Rakic, P.S., Wang, X.J., 2000. Synaptic mechanisms and network dynamics underlying spatial working memory in a cortical network model. Cerebr. Cortex 10, 910–923.
Condé, F., Lund, J.S., Jacobowitz, D.M., Baimbridge, K.G., Lewis, D.A., 1994. Local circuit neurons immunoreactive for calretinin, calbindin D-28k or parvalbumin in monkey prefrontal cortex: distribution and morphology. J. Comp. Neurol. 341, 95–116.
Constantinidis, C., Goldman-Rakic, P.S., 2002. Correlated discharges among putative pyramidal neurons and interneurons in the primate prefrontal cortex. J. Neurophysiol. 88, 3487–3497.
Datta, D., Arnsten, A.F.T., 2019. Loss of prefrontal cortical higher cognition with uncontrollable stress: molecular mechanisms, changes with age, and relevance to treatment. Brain Sci. 9, 113.
Datta, D., Yang, S.T., Galvin, V.C., Solder, J., Luo, F., Morozov, Y.M., Arellano, J., Duque, A., Rakic, P., Arnsten, A.F.T., Wang, M., 2019. Noradrenergic α1-adrenoceptor actions in the primate dorsolateral prefrontal cortex. J. Neurosci. 39, 2722–2734.
Datta, D., Perone, I., Morozov, Y., Arellano, J., Duque, A., Rakic, P., van Dyck, C., Arnsten, A.F.T., 2023. Localization of PDE4D, HCN1 channels and mGluR3 in rhesus macaque entorhinal cortex may confer vulnerability in Alzheimer's Disease. Cereb. Cortex 33, 11501–11516.
Datta, D., Yang, S., Joyce, M.K., Krienen, F.M., Wang, M., Arnsten, A.F.T., 2024. Key roles of CACNA1C/Cav1.2 and CALB1/calbindin in prefrontal neurons altered in cognitive disorders. JAMA Psych. in press.
Dazzi, L., Ladu, S., Spiga, F., Vacca, G., Rivano, A., Pira, L., Biggio, G., 2002. Chronic treatment with imipramine or mirtazapine antagonizes stress- and FG7142-induced increase in cortical norepinephrine output in freely moving rats. Synapse 43, 70–77.
Dębiec J, B.D., LeDoux, J.E., 2011. Noradrenergic enhancement of reconsolidation in the amygdala impairs extinction of conditioned fear in rats–a possible mechanism for the persistence of traumatic memories in PTSD. Depress. Anxiety 28, 86–93.
DeFelipe, J., 1997. Types of neurons, synaptic connections and chemical characteristics of cells immunoreactive for calbindin-D28K, parvalbumin and calretinin in the neocortex. J. Chem. Neuroanat. 14, 1–19.

Dorow, R., Horowski, R., Pashelke, G., Amin, M., Braestrup, C., 1983. Severe anxiety induced by FG7142, a B-carboline ligand for benzodiazepine receptors. Lancet 2, 98–99.
Driesen, N.R., Leung, H.C., Calhoun, V.D., Constable, R.T., Gueorguieva, R., Hoffman, R., Skudlarski, P., Goldman-Rakic, P.S., Krystal, J.H., 2008. Impairment of working memory maintenance and response in schizophrenia: functional magnetic resonance imaging evidence. Biol. Psychiatr. 64, 1026–1034.
Elston, G.N., 2000. Pyramidal cells of the frontal lobe: all the more spinous to think with. J. Neurosci. 20, RC95.
Elston, G.N., Benavides-Piccione, R., Elston, A., Manger, P.R., Defelipe, J., 2011. Pyramidal cells in prefrontal cortex of primates: marked differences in neuronal structure among species. Front. Neuroanat. 5, 2.
File, S.E., Pellow, S., Braestrup, C., 1985. Effects of the beta carboline, FG7142, in the social interaction test of anxiety and the holeboard: correlations between behavior and plasma concentrations. Pharmacol. Biochem. Behav. 22, 941–944.
Finlay, J.M., Zigmond, M.J., Abercrombie, E.D., 1995. Increased dopamine and norepinephrine release in medial prefrontal cortex induced by acute and chronic stress: effects of diazepam. Neuroscience 64, 619–628.
Fortaleza, E.A., Scopinho, A.A., Corrêa, F.M., 2012. B-adrenoceptors in the medial amygdaloid nucleus modulate the tachycardiac response to restraint stress in rats. Neuroscience 227, 170–179. https://doi.org/10.1016/j.neuroscience.2012.09.048.
Fu, A., Li, X., Zhao, B., 2008. Role of beta1-adrenoceptor in the basolateral amygdala of rats with anxiety-like behavior. Brain Res. 1211, 85–92.
Funahashi, S., Bruce, C.J., Goldman-Rakic, P.S., 1989. Mnemonic coding of visual space in the monkey's dorsolateral prefrontal cortex. J. Neurophysiol. 61, 331–349.
Funahashi, S., Chafee, M.V., Goldman-Rakic, P.S., 1993. Prefrontal neuronal activity in rhesus monkeys performing a delayed anti-saccade task. Nature 365, 753–756.
Gamo, N.J., Lur, G., Higley, M.J., Wang, M., Paspalas, C.D., Vijayraghavan, S., Yang, Y., Ramos, B.P., Peng, K., Kata, A., et al., 2015. Stress impairs prefrontal cortical function via D1 dopamine receptor interactions with HCN channels. Biol. Psychiatr. 78, 860–870.
George, M.S., Taylor, J.J., Short, E.B., 2013. The expanding evidence base for rTMS treatment of depression. Curr. Opin. Psychiatr. 26, 13–18.
Georgiades, A., Almuqrin, A., Rubinic, P., Mouhitzadeh, K., Tognin, S., Mechelli, A., 2023. Psychosocial stress, interpersonal sensitivity, and social withdrawal in clinical high risk for psychosis: a systematic review. Schizophrenia (Heidelb) 9, 38. https://doi.org/10.1038/s41537-023-00362-z.
Ghiasvand M, R.A., Ahmadi, S., Zarrindast, M.R., 2011. β1-noradrenergic system of the central amygdala is involved in state-dependent memory induced by a cannabinoid agonist, WIN55,212-2, in rat. Behav. Brain Res. 225, 1–6.
Glantz, L.A., Lewis, D.A., 2000. Decreased dendritic spine density on prefrontal cortical pyramidal neurons in schizophrenia. Arch. Gen. Psychiatr. 57, 65–73.
Glass, D.C., Reim, B., Singer, J.E., 1971. Behavioral consequences of adaptation to controllable and uncontrollable noise. J. Exp. Soc. Psychol. 7, 244–257.
Goldman-Rakic, P., 1995. Cellular basis of working memory. Neuron 14, 477–485.
Gomis-Vicent, E., Thoma, V., Turner, J.J.D., Hill, K.P., Pascual-Leone, A., 2019. Review: non-invasive brain stimulation in behavioral addictions: insights from direct comparisons with substance use disorders. Am. J. Addict. 28, 431–454. https://doi.org/10.1111/ajad.12945.
González-Burgos, G., Barrionuevo, G., Lewis, D.A., 2000. Horizontal synaptic connections in monkey prefrontal cortex: an in vitro electrophysiological study. Cerebr. Cortex 10, 82–92.
González-Burgos, G., Krimer, L.S., Povysheva, N.V., Barrionuevo, G., Lewis, D.A., 2005. Functional properties of fast spiking interneurons and their synaptic connections with pyramidal cells in primate dorsolateral prefrontal cortex. J. Neurophysiol. 93, 942–953.
Harnett, N.G., van Rooij, S.J.H., Ely, T.D., Lebois, L.A.M., Murty, V.P., Jovanovic, T., Hill, S.B., Dumornay, N.M., Merker, J.B., Bruce, S.E., et al., 2021. Prognostic neuroimaging biomarkers of trauma-related psychopathology: resting-state fMRI shortly after trauma predicts future PTSD and depression symptoms in the AURORA study. Neuropsychopharmacology 46, 1263–1271.
Hart, H., Lim, L., Mehta, M.A., Chatzieffraimidou, A., Curtis, C., Xu, X., Breen, G., Simmons, A., Mirza, K., Rubia, K., 2017. Reduced functional connectivity of fronto-parietal sustained attention networks in severe childhood abuse. PLoS One 12, e0188744.
Hartley, L.R., Adams, R.G., 1974. Effect of noise on the Stroop test. J. Exp. Psychol. 102, 62–66.
Hermans, E.J., van Marle, H.J., Ossewaarde, L., Henckens, M.J., Qin, S., van Kesteren, M. T., Schoots, V.C., Cousijn, H., Rijpkema, M., Oostenveld, R., Fernández, G., 2011. Stress-related noradrenergic activity prompts large-scale neural network reconfiguration. Science 334, 1151–1153.
Hockey, G.R.J., 1970. Effect of loud noise on attentional selectivity. Q. J. Exp. Psychol. 22, 28–36.
Hof, P.R., Morrison, J.H., 1991. Neocortical neuronal subpopulations labeled by a monoclonal antibody to calbindin exhibit differential vulnerability in Alzheimer's disease. Exp. Neurol. 111, 293–301.
Holmes, S.E., Scheinost, D., DellaGioia, N., Davis, M.T., Matuskey, D., Pietrzak, R.H., Hampson, M., Krystal, J.H., Esterlis, I., 2018. Cerebellar and prefrontal cortical alterations in PTSD: structural and functional evidence. Chronic Stress 2, 10.
Holmes, S.E., Scheinost, D., Finnema, S.J., Naganawa, M., Davis, M.T., DellaGioia, N., Nabulsi, N., Matuskey, D., Angarita, G.A., Pietrzak, R.H., et al., 2019. Lower synaptic density is associated with depression severity and network alterations. Nat. Commun. 1529.
Holt, C.E., Martin, K.C., Schuman, E.M., 2019. Local translation in neurons: visualization and function. Nat. Struct. Mol. Biol. 26, 557–566. https://doi.org/10.1038/s41594-019-0263-5.
Jacobsen, C.F., 1936. Studies of cerebral function in primates. Comp. Psychol. Monogr. 13, 1–68.
Johansson, L., Guo, X., Hällström, T., Norton, M.C., Waern, M., Ostling, S., Bengtsson, C., Skoog, I., 2013. Common psychosocial stressors in middle-aged women related to longstanding distress and increased risk of Alzheimer's disease: a 38-year longitudinal population study. BMJ Open 3, e003142.
Joyce, M.K., Garcia-Cabezas, M.A., John, Y., Barbas, H., 2020. Serial prefrontal pathways are positioned to balance cognition and emotion in primates. J. Neurosci. 40, 8306–8328.
Kritzer, M.F., Goldman-Rakic, P.S., 1995. Intrinsic circuit organization of the major layers and sublayers of the dorsolateral prefrontal cortex in the rhesus monkey. J. Comp. Neurol. 359, 131–143.
Lee, M., Mueller, A., Moore, T., 2020. Differences in noradrenaline receptor expression across different neuronal subtypes in macaque frontal eye field. Front. Neuroanat. 14, 574130 https://doi.org/10.3389/fnana.2020.574130.
Leidenheimer, N.J., Schechter, M.D., 1988. Discriminative stimulus control by the anxiogenic b-carboline FG7142: generalization to a physiological stressor. Pharmacol. Biochem. Behav. 30, 351–355.
Li, C., Sun, T., Zhang, Y., Gao, Y., Sun, Z., Li, W., Cheng, H., Gu, Y., Abumaria, N., 2023. A neural circuit for regulating a behavioral switch in response to prolonged uncontrollability in mice. Neuron 111, 2727–2741.e2727. https://doi.org/10.1016/j.neuron.2023.05.023.
Liston, C., McEwen, B.S., Casey, B.J., 2009. Psychosocial stress reversibly disrupts prefrontal processing and attentional control. Proc Nat Acad Sci USA 106, 912–917.
Liu, Y., Liang, X., Ren, W.W., Li, B.M., 2014. Expression of β1- and β2-adrenoceptors in different subtypes of interneurons in the medial prefrontal cortex of mice. Neuroscience 257, 149–157.
Luo, F., Zheng, J., Sun, X., Tang, H., 2017. Inward rectifier K+ channel and T-type Ca2+ channel contribute to enhancement of GABAergic transmission induced by β1-adrenoceptor in the prefrontal cortex. Exp. Neurol. 288, 51–61.
Luo Y, L.Z., Tu, Q., Xia, L., 2020. Metoprolol decreases retention of fear memory and facilitates long-term depression in lateral amygdala. Behav. Pharmacol. 31, 535–543.
Mazure, C.M. (Ed.), 1995. Does Stress Cause Psychiatric Illness?. American Psychiatric Press.
Medalla, M., Mo, B., Nasar, R., Zhou, Y., Park, J., Luebke, J.I., 2023. Comparative features of calretinin, calbindin, and parvalbumin expressing interneurons in mouse and monkey primary visual and frontal cortices. J Comp Neurol epub June 26.
Murchison CF, S.K., Jin, S.H., Thomas, S.A., 2011. Norepinephrine and ß1-adrenergic signaling facilitate activation of hippocampal CA1 pyramidal neurons during contextual memory retrieval. Neuroscience 181, 109–116.
Murphy, B.L., Arnsten, A.F.T., Goldman-Rakic, P.S., Roth, R.H., 1996. Increased dopamine turnover in the prefrontal cortex impairs spatial working memory performance in rats and monkeys. Proc. Natl. Acad. Sci. U.S.A. 93, 1325–1329.
Nakane, H., Shimizu, N., Hori, T., 1994. Stress-induced norepinephrine release in the rat prefrontal cortex measured by microdialysis. Am. J. Physiol. 267, R1559–R1566.
Ninan, P.T., Insel, T.M., Cohen, R.M., Cook, J.M., Skolnick, P., Paul, S.M., 1982. Benzodiazepine receptor-mediated experimental anxiety in primates. Science 218, 1332–1334.
Nook, E.C., Dodell-Feder, D., Germine, L.T., Hooley, J.M., DeLisi, L.E., Hooker, C.I., 2018. Weak dorsolateral prefrontal response to social criticism predicts worsened mood and symptoms following social conflict in people at familial risk for schizophrenia. Neuroimage 18, 40–50.
Pellow, S., File, S.E., 1986. Anxiolytic and anxiogenic drug effects on exploratory activity in an elevated plus-maze: a novel test of anxiety in the rat. Pharmacol. Biochem. Behav. 24, 525–529.
Perlstein, W.M., Carter, C.S., Noll, D.C., Cohen, J.D., 2001. Relation of prefrontal cortex dysfunction to working memory and symptoms in schizophrenia. Am. J. Psychiatr. 158, 1105–1113.
Peters, A., Palay, S.L., Webster, H.D., 1991. The Fine Structure of the Nervous System: Neurons and Their Supporting Cells. Oxford Univ. Press.
Pitman, R.K., Rasmusson, A.M., Koenen, K.C., Shin, L.M., Orr, S.P., Gilbertson, M.W., Milad, M.R., Liberzon, I., 2012. Biological studies of post-traumatic stress disorder. Nat. Rev. Neurosci. 13, 769–787. https://doi.org/10.1038/nrn3339.
Qin, S., Hermans, E.J., van Marle, H.J.F., Lou, J., Fernandez, G., 2009. Acute psychological stress reduces working memory-related activity in the dorsolateral prefrontal cortex. Biol. Psychiatr. 66, 25–32.
Qin, S., Cousijn, H., Rijpkema, M., Luo, J., Franke, B., Hermans, E.J., Fernández, G., 2012. The effect of moderate acute psychological stress on working memory-related neural activity is modulated by a genetic variation in catecholaminergic function in humans. Front. Integr. Neurosci. 6, 16.
Ramos, B., Colgan, L.A., Nou, E., Arnsten, A.F.T., 2008. β2 adrenergic agonist, clenbuterol, enhances working memory performance in aging rats and monkeys. Neurobiol. Aging 29, 1060–1069.
Rao, S.G., Williams, G.V., Goldman-Rakic, P.S., 1999. Isodirectional tuning of adjacent interneurons and pyramidal cells during working memory: evidence for microcolumnar organization in PFC. J. Neurophysiol. 81, 1903–1916.
Rao, S.G., Williams, G.V., Goldman-Rakic, P.S., 2000. Destruction and creation of spatial tuning by disinhibition: GABA(A) blockade of prefrontal cortical neurons engaged by working memory. J. Neurosci. 20, 485–494.
Rincón-Cortés, M., Herman, J.P., Lupien, S.J., Maguire, J., Shansky, R.M., 2019. Stress: influence of sex, reproductive status and gender. Neurobiol Stress 10, 100155.
Roozendaal, B., McGaugh, J.L., 2011. Memory modulation. Behav. Neurosci. 125, 797–824.

Roozendaal, B., McReynolds, J.R., McGaugh, J.L., 2004a. The basolateral amygdala interacts with the medial prefrontal cortex in regulating glucocorticoid effects on working memory impairment. J. Neurosci. 24, 1385–1392.
Roozendaal, B., de Quervain, D.J., Schelling, G., McGaugh, J.L., 2004b. A systemically administered beta-adrenoceptor antagonist blocks corticosterone-induced impairment of contextual memory retrieval in rats. Neurobiol. Learn. Mem. 81, 150–154.
Rotaru, D.C., Yoshino, H., Lewis, D.A., Ermentrout, G.B., Gonzalez-Burgos, G., 2011. Glutamate receptor subtypes mediating synaptic activation of prefrontal cortex neurons: relevance for schizophrenia. J. Neurosci. 31, 142–156.
Roth, R.H., Tam, S.-Y., Ida, Y., Yang, J.-X., Deutch, A.Y., 1988. Stress and the mesocorticolimbic dopamine systems. Ann. NY Acad. Sci. 537, 138–147.
Roullet, P., Vaiva, G., Véry, E., Bourcier, A., Yrondi, A., Dupuch, L., Lamy, P., Thalamas, C., Jasse, L., El Hage, W., Birmes, P.T., 2021. Traumatic memory reactivation with or without propranolol for PTSD and comorbid MD symptoms: a randomised clinical trial. Neuropsychopharmacology 46, 1643–1649.
Roussy M, L.R., Duong, L., Corrigan, B., Gulli, R.A., Nogueira, R., Moreno-Bote, R., Sachs, A.J., Palaniyappan, L., Martinez-Trujillo, J.C., 2021. Ketamine disrupts naturalistic coding of working memory in primate lateral prefrontal cortex networks. Mol. Psychiatr. 26, 6688–6703.
Schindelin, J., Arganda-Carreras, I., Frise, E., Kaynig, V., Longair, M., Pietzsch, T., Preibisch, S., Rueden, C., Saalfeld, S., Schmid, B., et al., 2012. Fiji: an open-source platform for biological-image analysis. Nat. Methods 9, 676–682. https://doi.org/10.1038/nmeth.2019.
Schroeter, M.L., Vogt, B., Frisch, S., Becker, G., Barthel, H., Mueller, K., Villringer, A., Sabri, O., 2012. Executive deficits are related to the inferior frontal junction in early dementia. Brain 135, 201–215.
Seo, D.O., Zhang, E.T., Piantadosi, S.C., Marcus, D.J., Motard, L.E., Kan, B.K., Gomez, A. M., Nguyen, T.K., Xia, L., Bruchas, M.R., 2021. A locus coeruleus to dentate gyrus noradrenergic circuit modulates aversive contextual processing. Neuron 109, 2116–2130.e2116. https://doi.org/10.1016/j.neuron.2021.05.006.
Sevastre-Berghian, A.C., Toma, V.A., Sevastre, B., Hanganu, D., Vlase, L., Benedec, D., Oniga, I., Baldea, I., Olteanu, D., Moldovan, R., et al., 2018. Characterization and biological effects of Hypericum extracts on experimentally-induced - anxiety, oxidative stress and inflammation in rats. J. Physiol. Pharmacol. 69, 789–800.
Sinha, R., 2007. The role of stress in addiction relapse. Curr. Psychiatr. Rep. 9, 388–395.
Smith, K., Lacadie, C.M., Milivojevic, V., Fogelman, N., Sinha, R., 2023. Sex differences in neural responses to stress and drug cues predicts future drug use in individuals with substance use disorder. Drug Alcohol Depend. 244, 109794 https://doi.org/10.1016/j.drugalcdep.2023.109794.
Southwick, S.M., Krystal, J.H., Morgan, C.A., Johnson, D., Nagy, L.M., Nicolaou, A., Heninger, G.R., Charney, D.S., 1993. Abnormal noradrenergic function in posttraumatic stress disorder. Arch. Gen. Psychiatr. 50, 266–274.
Southwick, S.M., Bremner, J.D., Rasmusson, A., Morgan, C.A.r., Arnsten, A., Charney, D. S., 1999. Role of norepinephrine in the pathophysiology and treatment of posttraumatic stress disorder. Biol. Psychiatr. 46, 1192–1204.
Szczepanski, S.M., Knight, R.T., 2014. Insights into human behavior from lesions to the prefrontal cortex. Neuron 83, 1002–1018.
Takamatsu, H., Noda, A., Kurumaji, A., Murakami, Y., Tatsumi, M., Ichise, R., Nishimura, S., 2003. A PET study following treatment with a pharmacological stressor, FG7142, in conscious rhesus monkeys. Brain Res. 980, 275–280.
Torres-Gomez, S., Blonde, J., Mendoza-Halliday, D., Kuebler, E., Everest, M., Wang, X.-J., Inoue, W., Poulter, M., Martinez-Trujillo, J., 2020. Changes in the proportion of inhibitory interneuron types from sensory to executive areas of the primate neocortex. Implications for the origins of working memory representations. Cerebr. Cortex 30, 4544–4562.
Vijayraghavan, S., Wang, M., Birnbaum, S.G., Bruce, C.J., Williams, G.V., Arnsten, A.F.T., 2007. Inverted-U dopamine D1 receptor actions on prefrontal neurons engaged in working memory. Nat. Neurosci. 10, 376–384.
Weinberger, D.R., Berman, K.F., Zec, R.F., 1986. Physiologic dysfunction of dorsolateral prefrontal cortex in schizophrenia. I. Regional cerebral blood flow evidence. Arch. Gen. Psychiatr. 43, 114–124.
Weitl, N., Seifert, R., 2008. Distinct interactions of human beta1- and beta2-adrenoceptors with isoproterenol, epinephrine, norepinephrine, and dopamine. J. Pharmacol. Exp. Therapeut. 27, 760–769.
Zerbi, V., Floriou-Servou, A., Markicevic, M., Vermeiren, Y., Sturman, O., Privitera, M., von Ziegler, L., Ferrari, K.D., Weber, B., De Deyn, P.P., et al., 2019. Rapid reconfiguration of the functional connectome after chemogenetic locus coeruleus activation. Neuron 103, 702–718. https://doi.org/10.1016/j.neuron.2019.05.034 e705.